BULK TITANIUM MICRONEEDLES WITH EMBEDDED MICROFLUIDIC NETWORKS FOR TRANSDERMAL DRUG DELIVERY

E. R. Parker, M. P. Rao, K. L. Turner, and N. C. MacDonald
Mechanical and Environmental Engineering
University of California, Santa Barbara, California, USA

ABSTRACT

Recent developments have allowed for the bulk micromachining of titanium for MEMS applications. Biomedical microsystems in particular can benefit from the high fracture toughness and biocompatibility associated with titanium. This paper reports on the design and fabrication of an in-plane, bulk titanium microneedle device using multilayer lamination. Thin titanium foils are patterned, etched, and bonded together to form microneedle arrays. A microfluidic network embedded within these arrays allows for controlled fluid delivery through the device. This fabrication approach offers a novel, robust platform for transdermal drug delivery applications.

1. INTRODUCTION

Microfabrication techniques have been used for a number of applications in drug delivery including microneedle arrays capable of penetrating the outer layer of the epidermis and delivering fluids [1,2]. In general, microneedle devices can be classified as either out-of-plane or in-plane. Out-of-plane microneedles, where the needle length is typically defined by etch or mold depth, have been fabricated using a number of different materials, including single-crystal silicon [3-6], polymers [7], and electrodeposited metals [8]. In-plane microneedles systems, where the lengths of the needles are defined lithographically, have also used similar material systems including single-crystal silicon [9-11], polysilicon [12], and electrodeposited metals [13]. In this paper, we report on the fabrication and preliminary characterization of bulk titanium in-plane microneedles realized using recently developed high-aspect-ratio titanium micromachining and multilayer lamination technologies. This approach combines the benefits of bulk micromachining techniques with the high fracture toughness and proven biocompatibility of titanium, thus creating a robust, non-brittle platform for low-cost transdermal drug delivery and diagnostic applications.

Owing to its biocompatibility and fracture toughness, titanium has long been used for macro-scale implantable biomedical devices such as hip implants and pacemaker cases [14]. Now, with the advent of enabling micromachining technologies [15,16], the use of titanium can be expanded into micro-scale biomedical applications. Using these techniques, micrometer-sized features have been defined in both thick titanium substrates and thin titanium foils via inductively coupled plasma (ICP) dry etching [16]. The microfabrication of devices using titanium foils is especially advantageous because it allows for the development of three-dimensional architectures through the successive stacking and bonding of through-etched foils (i.e. multilayer lamination), resulting in robust, metallic microstructures fabricated from bulk material rather than deposited thin films. For this application, a microneedle array with embedded microfluidics is patterned onto a thin titanium foil and through-etched. This foil is then thermocompression bonded to a second titanium thin foil in order to seal the microfluidic networks. Fluid has been successfully pumped through these devices and they have been shown to survive initial insertion tests.

2. DESIGN AND FABRICATION

As described above, the bulk titanium microneedle devices are fabricated using two titanium thin foils. The first foil is patterned and etched to form the microneedle array structure with staggered microfluidic networks. This foil is then thermocompression bonded to a second foil and subsequently etched to form self-standing microneedles with embedded channels. Figure 1 outlines this process flow in more detail.

Prior to processing, the titanium thin foils (2.5x2.5 cm^2, 99.6% annealed, Goodfellow Corporation) are chemically mechanically polished (CMP) to reduce surface roughness. Following CMP, a TiO_2 masking layer is sputter deposited on both the front and backside of the foil and patterned on the front to define the microneedle array geometry. This oxide patterning is performed using a CHF_3 dry etch. A second lithography step is then used to define the microfluidic networks within the needle arrays. In order to create the embedded network geometry, this pattern is only partially transferred into the masking oxide. Next, a series of dry etches is used to through-etch the titanium foil to form the microneedle arrays with staggered microfluidic channels. A bulk titanium deep etch is used to etch approximately halfway into the depth of the thin foil surrounding the needle array. The titanium deep etch uses a Cl_2/Ar chemistry, as described in [16]. This is followed by an oxide etch required to clear the remaining masking oxide within the microfluidic network pattern. Finally, a second titanium deep etch is used to completely through-etch the titanium foil surrounding the microneedle array and define the channels. This series of etches can be performed continuously in the same ICP etch tool (Panasonic E640-ICP dry etching system, Panasonic Factory Solutions) without breaking vacuum, therefore reducing process time considerably.

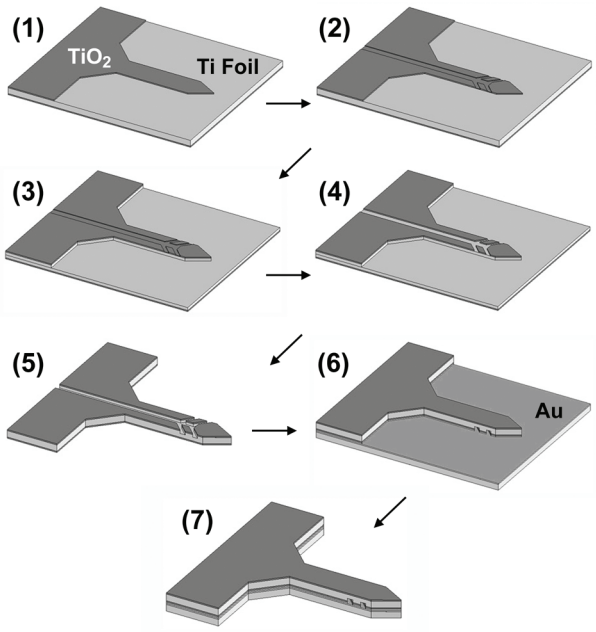

Figure 1: Bulk titanium microneedle process flow: (1) first oxide etch to define needle geometry; (2) second oxide etch to partially define embedded channels; (3) first deep etch; (4) third oxide etch to fully define embedded channels; (5) second deep etch to through-etch foil with staggered channel depths; (6) gold-gold thermocompression bonding to unpatterned foil (top foil is flipped); (7) final deep etch to through-etch bottom foil.

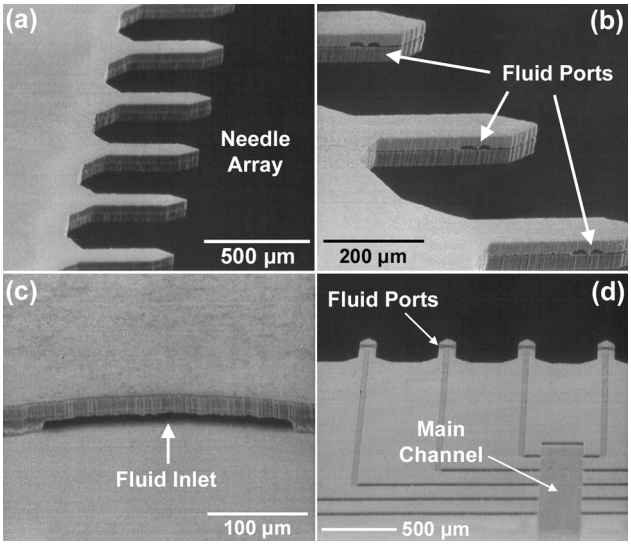

Figure 2: Scanning electron micrographs of: (a) bonded titanium thin foil needle array; (b) fluid side ports; (c) fluid inlet; and (d) embedded microfluidic networks prior to bonding. This microneedle array used two 25 µm titanium thin-foils. The pictured microneedles lengths are 500 µm long and 100 µm wide.

After the needle structure is fully defined in the first titanium thin foil, a 0.5-µm-thin gold layer is deposited using either sputtering or electron beam evaporation. A gold film of equal thickness is also deposited on a second unpatterned titanium thin foil. These foils are then bonded together in order to seal the microfluidic networks using thermocompression bonding. The first foil, with the backside TiO_2 deposited film now facing up, is then used as a mask to through-etch the bottom foil in a final titanium deep etch. The result of this process is a microneedle needle array comprised of two bonded titanium thin foils with integrated microfluidics.

The process described above offers a significant amount of design and process flexibility because: a) the needle length and shape are defined lithographically; b) needle rigidity can be easily controlled by varying the foil thicknesses (single foils from 25-100 µm have been through-etched); and c) the bonding requires no alignment as the top foil acts as a shadow mask during bottom foil etching. Moreover, the in-plane nature of the embedded fluid networks will also facilitate future integration of additional microfluidic components, such as pumps, filters, and sensors, which will provide increased device functionality.

Figure 2 shows several SEM images of a bulk titanium microneedle array fabricated using two 25 µm titanium thin foils. As mentioned previously, the thickness of one or both of these foils can be increased if additional needle rigidity is required. The microneedles shown in Fig. 2 are 500 µm long with a 30º tip angle. We have also fabricated additional tip designs (15º and 45º) and needle lengths (750 and 1000 µm). Fluid delivery by the microneedles shown in Fig. 2 is via two side ports on either side of the structure. Single ports designed to terminate at the tip of the microneedle structure have also been designed and fabricated. Currently, the fluid ports are approximately 25 µm wide, as controlled by lithography, and 10 µm tall, as controlled by the etch depth of the embedded channels. Thicker titanium foils would enable these channels to be etched deeper, thus further increasing overall fluid capacity within the device.

In order to minimize fluid pressure within the device and ensure uniform flow distribution to each microneedle in the array, simulations were used to optimize the embedded microfluidic network design. Figure 3 shows a representative simulation of the velocity profile through a microfluidic network design for an inlet volumetric flow rate of 100 µL/min. In addition to microfluidic considerations, several device factors were used to determine the most appropriate channel pattern. First, in order to simplify the device interface, fluid is distributed to all microneedles via a single inlet. Second, the maximum channel width was limited to 250 µm to ensure that the structure would not collapse during the bonding step. Finally, dense packing was avoided because the accompanying reduction of bonding area between the channels might detrimentally effect reliability.

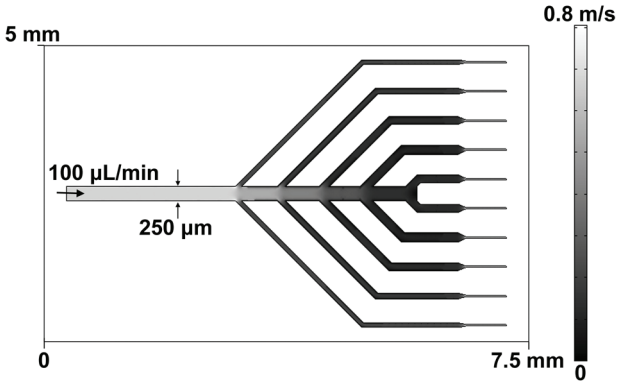

Figure 3: Representative simulation of the velocity profile through the embedded microfluidic network for a ten microneedle array. FEMLAB has been used to optimize flow distribution and to minimize internal pressure across the device as a function of inlet flow rate.

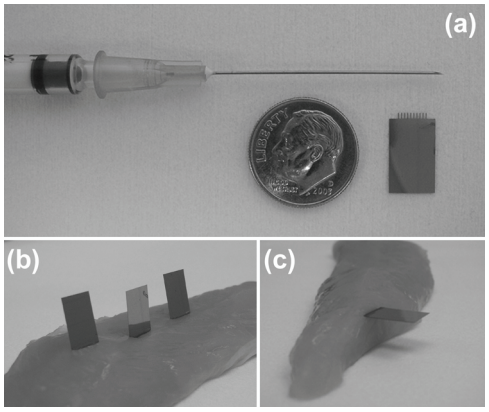

Figure 4: (a) The titanium microneedle array chip shown next to a dime and a typical hypodermic needle; (b) (from left to right) 500, 750, and 1000 µm microneedle arrays inserted into a chicken breast; and (c) side view of the 1000 µm microneedle array reinserted into the chicken breast.

3. RESULTS

Following fabrication, several preliminary experiments were performed to characterize the robustness of the bulk titanium microneedle devices. These included multiple insertion tests into various materials to determine potential mechanical failures and qualitative fluid testing at various volumetric flow rates. As shown in Fig. 4a, the completed device is smaller than a dime and yet can still be handled easily. In addition, this size is completely scalable to a specific requirement. For example, initially all arrays were comprised of ten microneedles. However, the bulk titanium platform would be robust enough to handle a 100 microneedle array, if so desired. As shown in Figs. 4b and c, microneedle arrays of 500 µm, 750 µm, and 1000 µm lengths can be inserted and reinserted without critical buckling failure or bond delamination.

For fluid delivery experiments, the titanium microneedle chip can be interfaced to a syringe pump either by mounting it to a plexiglass stage or by attaching tubing directly to the device via epoxy. Figure 5 shows fluid pumping through the titanium device while mounted onto the stage. For higher flow rate experiments, it was found that directly adhering tubing to the device eliminated leakage issues encountered with the stage. However, for low flow rate experiments the stage was easiest because the device was not permanently attached and could be removed, cleaned, and reused. Figure 5b shows the microneedle array inserted into acrylamide gel, a polymer matrix commonly used for gel electrophoresis. The transparency of this gel allows for real time monitoring of fluid delivery. Figure 5c shows droplets formed at the ends of the microneedles with fluid pumping. For this array, fluid ports were designed to be at the tips of the microneedles.

Current research focuses on more comprehensive fluidic and mechanical characterization of the microneedle arrays. This includes measuring the pressure drop across the device as a function of inlet volumetric flow rate. This test

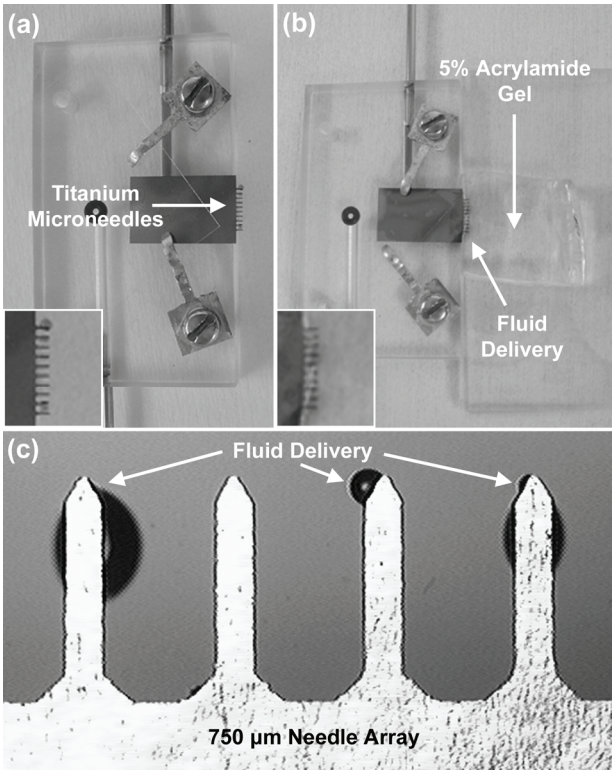

Figure 5: (a) The titanium microneedles can be mounted onto a plexiglass stage interfaced with a syringe pump to control fluid flow (inset showing close-up of fluid droplets emanating from needle tips). (b) Real time fluid delivery can be observed using 5% acrylamide gel (inset showing close-up of needles inserted into gel with fluid pumping). (c) Using an optical microscope, fluid delivery through 750 µm microneedle arrays with tip ports can be easily imaged.

is being performed to determine the effect of the embedded microfluidic network design and etch depth on internal pressure. The mechanical modeling and characterization of these microneedle arrays as a function of foil thickness and needle length is also being performed. In the future, we plan to integrate additional microfluidic components including an on-chip pumping mechanism to eliminate the need for external pumping.

4. CONCLUSIONS

A novel and robust platform for transdermal drug delivery has been fabricated using recently developed bulk titanium micromachining technologies. The high fracture toughness and biocompatibility of titanium makes it an ideal material system for microneedle applications. The fabricated devices are comprised of two thermocompression-bonded thin titanium foils with integrated microfluidics. This process offers a significant amount of design flexibility, including the lithographic control of needle length and shape and the ability to control needle rigidity by foil thickness. In the future, the device design will also allow for additional microfluidic component integration, such as micropumps or sensors.

5. ACKNOWLEDGEMENTS

The authors would like to thank Professor Carl D. Meinhart for his help with microfluidic simulations and Yanting Zhang for her help with fluidic characterization. This research was funded by DARPA-MTO.

6. REFERENCES

[1] D. V. McAllister, M. G. Allen, and M. R. Prausnitz, "Microfabricated Microneedles for Gene and Drug Delivery," *Annu. Rev. Biomed. Eng.*, vol. 2, pp. 289-313, 2000.

[2] M. L. Reed and W.-K. Lei, "Microsystems for Drug and Gene Delivery," *P. IEEE*, vol. 92, no. 1, pp. 56-75, 2004.

[3] P. Griss and G. Stemme, "Side-Opened Out-of-Plane Microneedles for Microfluidic Transdermal Liquid Transfer," *J. Microelectromech. Syst.*, vol. 12, no. 3, pp. 296-301, 2003.

[4] H. J. G. E. Gardeniers, R. Luttge, E. J. Berenschot, M. J. de Boer, S. Y. Yeshurun, M. Hefetz, R. van't Oever, and A. van den Berg, "Silicon Micromachined Hollow Microneedles for Transdermal Liquid Transport," *J. Microelectromech. Syst.*, vol. 12, no. 6, pp. 855-862, 2003.

[5] E. V. Mukerjee, S. D. Collins, R. R. Isseroff, and R. L. Smith, "Microneedle Array for Transdermal Biological Fluid Extraction and In Situ Analysis," *Sensor Act. A*, vol. 114, pp. 267-275, 2004.

[6] B. Stoeber and D. Liepmann, "Arrays of Hollow Out-of-Plane Microneedles for Drug Delivery," *J. Microelectromech. Syst.*, vol. 14, no. 3, pp. 472-479, 2005.

[7] J.-H. Park, M. G. Allen, and M. R. Praunitz, "Biodegradable Polymer Microneedles: Fabrication, Mechanics, and Transdermal Drug Delivery," *J. Control. Release*, vol. 104, pp. 51-66, 2005.

[8] S. P. Davis, W. Martanto, M. G. Allen, and M. R. Praunitz, "Hollow Metallic Microneedles for Insulin Delivery to Diabetic Rats," *IEEE Trans. Biomed. Eng.*, vol. 52, no. 5, pp. 909-915, 2005.

[9] L. W. Lin and A. P. Pisano, "Silicon-Processed Microneedles," *J. Microelectromech. Syst.*, vol. 8, no. 1, pp. 78-84, 1999.

[10] J. K. Chen, K. D. Wise, J. F. Hetke, and S. C. Bledsoe, "A Multichannel Neural Probe for Selective Chemical Delivery at the Cellular Level," *IEEE Trans. Biomed. Engr.*, vol. 44, no. 8, pp. 760-769, 1997.

[11] S.-J. Paik, S. Byun, J.-M. Lim, Y. Park, A. Lee, S. Chung, J. Chang, K. Chun, and D. Cho, "In-Plane Single-Crystal-Silicon Microneedles for Minimally Invasive Microfluid Systems," *Sensor Act. A*, vol. 114, pp. 276-284, 2004.

[12] J. D. Zahn, N. H. Talbot, D. Liepmann, and A. P. Pisano, "Microfabricated Polysilicon Microneedles for Minimally Invasive Biomedical Devices," *Biomed. Microdev.*, vol. 2, pp. 295-303, 2000.

[13] S. Chandrasekaran, J. D. Brazzle, and A. B. Frazier, "Surface Micromachined Metallic Microneedles," *J. Microelectromech. Syst.*, vol. 12, no. 3, pp. 281-288, 2003.

[14] D. M. Brunette, P. Tengvall, M. Textor, and P. Thomsen, *Titanium in Medicine: Material Science, Surface Science, Engineering, Biological Responses, and Medical Applications*, Springer, Berlin, 2001.

[15] M. F. Aimi, M. P. Rao, N. C. MacDonald, A. S. Zuruzi, and D. Bothman, "High-Aspect-Ratio Bulk Micromachining of Titanium," *Nature Materials*, vol. 3, no. 2, pp 103-105, 2004.

[16] E. R. Parker, B. J. Thibeault, M. F. Aimi, M. P. Rao, and N. C. MacDonald, "Inductively Coupled Plasma Etching of Bulk Titanium for MEMS Applications," *J. Electrochem. Soc.*, vol. 152, no. 10, pp. 675-683, 2005.